




Cite this: *RSC Appl. Polym.*, 2025, **3**, 268

## Photocurable epoxy-based composite for rapid orthopedic soft casting†

Beatrice Tosetto,<sup>a,b,c</sup> Roberto Mo,<sup>c</sup> Candido Fabrizio Pirri<sup>a,c</sup> and Ignazio Roppolo <sup>\*a,c</sup>

Since the last century, plaster of Paris bandages have been the gold standard for orthopedic casting. Despite their extensive use, they have several drawbacks in day-to-day life, such as high weight and sensitivity to water. Moreover, they can cause skin burns, pressure sores, and other complications. Consequently, the urgency to propose alternative materials to solve these problems has emerged in the last decades, leading to the so-called soft casts, especially in pediatric orthopedics. In this context, a photocurable composite, based on the impregnation of a medical net with epoxy resins, is presented here. The impregnated medical net was rapidly transformed into a rigid device by means of visible light irradiation with an ad-hoc designed LED lamp (410–420 nm). Reaction activation was shifted to the visible range by exploiting isopropyl-9H-thioxanthen-9-one (ITX) as the photosensitizer, and the composites' polymerization was evaluated *via* FT-IR analyses and thermal camera monitoring. The composites were also tested through tensile and three-point bending tests, revealing a stiffness comparable to that of soft casts already on the market. Compared to commercially available photocurable casts, this work introduces two key innovations: first, the employment of commercially available epoxy resins (monomer: 3,4-epoxycyclohexylmethyl 3,4-epoxycyclohexanecarboxylate), which enables avoiding the problems of oxygen inhibition; second, the use of a tubular medical net that is stretchable along the transversal direction, which is already used in the medical field for medication positioning. This latter advancement simplifies the application process compared to conventional techniques, making the obtained casts easy and fast to apply, light and breathable, thus maintaining promising properties for orthopedic rapid soft casts.

Received 9th August 2024,  
Accepted 3rd December 2024

DOI: 10.1039/d4lp00248b

rsc.li/rscappliedpolym

## Introduction

Since the mid-19<sup>th</sup> century, plaster of Paris (POP) has been commonly used for immobilizing fractured bones. From 1852 to now, many innovations have characterized this orthopedic device, both in cast manufacturing and in the materials employed, with the introduction of advanced materials such as fiberglass and thermoplastic casts. In this context, a fiberglass cast consists of a tape impregnated with polyurethane that can be activated in water, while a thermoplastic cast is a thermoplastic sheet that can be softened in hot water at 70–75 °C and molded on the patient. Despite these innovations, POP bandages are still the most used materials

because they are cheaper and standardly covered by insurance schemes, followed by fiberglass casts (FGCs).<sup>1</sup> Nevertheless, they present several drawbacks such as the time required to achieve optimum performances; the high weight of the casts; low breathability, which leads to itching and redness; the impossibility of becoming wet; and the fact that the efficacy and safety of the casts rely on operator expertise during their application. In fact, the standard procedure consists of placing the limb in a proper position depending on the injury, followed by wetting the bandage roll by dipping it into water to activate its hardening and finally wrapping the bandage around the fractured limb in an appropriate number of layers (5–12 for POP and 4–6 for FGC), without causing any change in the limb position. Furthermore, all the procedures must be performed quickly because the material will harden in 3–8 minutes.<sup>1,2</sup> Consequently, casts must be only applied by practiced orthopedic technicians or doctors, but still, the procedure results in complications and injuries such as skin burns and pressure sores that can appear due to improper roll soaking, poor casting technique, or due to movements before complete hardening. In the latter case, the short casting windows may hinder the correct application.<sup>1,3,4</sup> Another

<sup>a</sup>Department of Applied Science and Technology, Politecnico di Torino, Corso Duca degli Abruzzi 24, Turin 10129, Italy. E-mail: ignazio.roppolo@polito.it

<sup>b</sup>Department of Chemistry, Biology and Biotechnology, University of Perugia, Via Elce di Sotto 8, 06123 Perugia, Italy

<sup>c</sup>Center for Sustainable Future Technologies, Italian Institute of Technology, Via Livorno 60, 10144 Turin, Italy

†Electronic supplementary information (ESI) available. See DOI: <https://doi.org/10.1039/d4lp00248b>



important drawback is the impossibility of monitoring the healing of the injured part by performing X-ray analyses without removing the cast since POP is radiopaque and, in FGC, fiberglass mesh patterns cause interference, attenuating the signal.<sup>1</sup> Finally, the immobilization techniques are often used in several other treatments such as Clubfoot and post-operative immobilization, but it was proven that POP and FGC have a stiffness well beyond sufficient one. This is particularly evident in pediatric orthopedics, where the soft casting technique (*i.e.* semi-rigid thermoplastic tape usually wrapped around the limb) results are proven and even more effective than those of the standard casting, thanks to a shorter rehabilitation time related to the patient's higher mobility with the cast.<sup>5–8</sup>

Consequently, the necessity of further evolution in the cast properties emerges clearly, and the required characteristics include but are not limited to, easy procedures to apply and remove the cast, fast hardening with a controllable hardening window, lightweight, radiotransparency, tunable rigidity, waterproof and breathability. Many of those characteristics were recently fulfilled by the use of photocurable casts.<sup>1</sup>

Photocurable casts are composed of a monomeric formulation that can be polymerized through light irradiation, resulting in a fast hardening. This allows the technicians to place the casts without rushing and close the cast windows when decided. Photocurable casts are already commercially available and are mainly based on combining acrylates and methacrylate with different kinds of specifically designed textile supports, made of glass fiber, nylon, PTFE, PET, rayon, or cotton.<sup>9–15</sup> Those casts have advantages related to curing speed and lightweight, however, similar to most radical polymerization processes, suffer from oxygen inhibition, *i.e.* the polymerization is quenched when in contact with oxygen.<sup>16–19</sup> This is obviously a strong limitation in view of cast application and it is necessary to confine the resins in volumes not in contact with oxygen, making the support design complex and typically leading to the subdivision of casts in sizes, limiting the customizability and the ability to fit the patient limb properly.<sup>9</sup> Different from (meth)acrylic resins, epoxy resins may be polymerized by a cationic photoinduced mechanism, which is not prone to oxygen inhibition.<sup>16,17,20–22</sup> In this context, the use of epoxy in casts can make the design simpler, more versatile and potentially applicable to everyday life. Moreover, epoxies give lower shrinkage during polymerization (5% *vs.* 10–15% for acrylates and methacrylates), which may represent a further advantage compared to more conventional photocurable casts, due to lower stresses and lower limb compression.<sup>18,19,22,23</sup> Nevertheless, epoxy resins have other drawbacks that must be overcome in view of the development of rapid photocurable orthopedic cast. The first one is that the cationic mechanism is slower than the radical polymerization; therefore, an optimization of the formulations and the curing conditions is crucial.<sup>20,23</sup> Furthermore, the available cationic photoinitiators can be mainly activated by UV light irradiation,<sup>24,25</sup> which can be hazardous for the human skin; consequently, a shift to visible light is strongly

recommended.<sup>26–28</sup> To this purpose, it is necessary to shift the absorption of the formulations towards higher wavelengths, and this is possible by employing photosensitizers (PhS).<sup>17,23,24,29</sup>

In this work, an innovative strategy is reported to develop photocurable soft casts employing a medical elastic and tubular net impregnated with epoxy resins. Among the possible monomers, cycloaliphatic epoxy resins (CE) are well-known for their good mechanical performance, high polymerization rate and lower tendency to yellowing when exposed to sunlight.<sup>23,30,31</sup> Furthermore, it does not contain bisphenol A. To obtain fast and visible-induced curing, as well as suitable mechanical properties, different photoinitiators (PhI) and photosensitizers (PhS) were studied, and the optimized formulation was then used to impregnate a medical net to obtain a rigid mesh after irradiation.<sup>32–36</sup> In this sense, the elastic medical net employed is already used for medication and consequently assures conformability when applied to human skin. Moreover, thanks to its tubular and transversally stretchable design, an easier application is guaranteed, compared to the standard cast application, which in turn leads to the possibility of dressing the net without requiring it to be wrapped around the limb. Finally, a desired number of net layers can be applied to the injured part, allowing better control of the mechanical properties of the soft cast.

In this study, photocurable composites were developed, showing promising results for the application of orthopedic rapid soft casts, and two main innovations are proposed: employing (i) epoxy resins and (ii) a tubular medical net stretchable along the transversal direction. These innovations facilitate the cast design compared to other photocurable casts and will simplify the application process compared to conventional techniques, making the obtained composites, light, breathable, and easy and fast to apply.

## Material and methods

### Material

The monomeric resin 3,4-epoxycyclohexylmethyl 3,4-epoxycyclohexanecarboxylate (CE) was purchased from abcr. The photoinitiators diphenyliodonium hexafluorophosphate (Iod I), (4-methylphenyl) [4-(2-methylpropyl)phenyl] iodonium hexafluorophosphate (Iod II), TEGO photocompound 1465 (T65), TEGO photocompound 1467 (T67), bis(4-*tert*-butylphenyl)iodonium hexafluorophosphate (BTB), and triarylsulfonium hexafluoroantimonate (Solf) were obtained from Basf, Evonik and Sigma Aldrich. The photosensitizers camphorquinone (C) and isopropyl-9*H*-thioxanthen-9-one, a mixture of 2- and 4-isomers (ITX) were purchased from Sigma Aldrich. All the employed chemicals were used as received. The medical net (Surgifix® Zerolatex) was provided by Fra Production SpA (Italy). The Fiberglass cast tape (Tomato Super Cast, Tomato Casting Tape), the Plaster of Paris bandage (Prontex, SAFETY SpA), and the cotton stockinette (Tubiton, Molnlycke Healthcare) were kindly provided by MD. Andrea Audisio.



## Method

**Polymeric and composite sample preparation.** The monomeric formulations were prepared by adding the photoinitiator and, eventually, the photosensitizer to the monomer CE (formulation composition reported in Tables 1, S1 and S2†) and sonicated until complete dispersion of the additives. 100 µm thin samples were obtained with a wire wound bar, while bulk polymeric samples (thickness: 3 mm) were obtained by casting. Composite samples were produced in different shapes: a strip or cylinder, single- or double-layer. In every case, 1 ml of resin with 10 cm<sup>2</sup> of mesh was poured on the medical net, and homogeneous impregnation was assisted by pressing with a roll, resulting in a monomer concentration in the composite of 85% (percent by weight). Then, the soaked net was placed on a preform that transversally stretched the mesh with the desired stretching level (eqn (1)).

$$\text{Final width} = \text{initial width} \times (1 + \text{stretching level}) \quad (1)$$

When multi-layer specimens were prepared, the desired number of soaked medical net layers were deposited. Finally, all the polymeric and composite samples were cured using light irradiation according to the parameters described in the text. Four different lamps were employed: UV(-01A) and broad-band white light (-03) Hamamatsu LC8 lamps, Solar Simulator (Newport, Oriel Instrument U.S.A., 91191A-1000), and an *ad-hoc* designed lamp operating with LS-XC06-S410-SD111 LEDs (Intelligent LED Solutions). Further details on the LED lamp design are reported in the ESI.† In the case of cylindrical samples cured with the *ad-hoc* design lamp, photocuring was

performed in three irradiation steps, rotating the lamp around the specimens. These steps overlap subsequent curing areas to avoid low polymerized transitions.

**Standard casts preparation.** Hollow cylindrical specimens (diameter: 5 cm, length: 25 cm) were fabricated with POP and FGC wrapped around a rigid tube by a registered orthopedic technician according to the manufacturer's requirement and conventional procedure. Those samples were used as a reference for mechanical properties.

**Polymerization characterization.** Fourier Transform Infrared Spectroscopy (FTIR-ATR) tests were performed with a Nicolet iS50 FTIR Spectrometer in the Attenuated Total Reflection mode with diamond crystal (32 scans from 4000 to 500 cm<sup>-1</sup>, resolution of 4.0 cm<sup>-1</sup>) on the not-irradiated soaked net and cross-linked composites. The polymerization was monitored by evaluating the area below the peak at 805–815 cm<sup>-1</sup> (related to asymmetric stretching vibrations of the epoxide ring) compared to the one under the peak at 1720–1730 cm<sup>-1</sup> (C=O bond stretch in the ester group).<sup>37–40</sup> The conversion degree (CD) was calculated using eqn (2):

$$CD = \left( 1 - \frac{\frac{A_{810}^{\text{composite}}}{A_{1725}^{\text{composite}}}}{\frac{A_{810}^{\text{soaked net}}}{A_{1725}^{\text{soaked net}}}} \right) \times 100 \quad (2)$$

where *A* is the area below the peaks at 805–815 cm<sup>-1</sup> and 1720–1730 cm<sup>-1</sup> evaluated for the composite and the soaked net. FTIR-ATR tests were performed on both sides of the composites at different times after the irradiation. For each experiment, the FT-IR spectrum was averaged from three measurements on different sample points.

The temperatures developed during light irradiation were monitored with a thermal camera on the irradiated surface and through thermal probes on the opposite side. The thermal camera employed is FLIR E6-XT (thermal resolution: 240 × 180 pixel; accuracy: ±2 °C or ±2%; thermal sensitivity/NETD < 0.06 °C/<60 mK; temperature range from –20 °C to 550 °C) and was placed at 30 cm from the analyzed surface. The thermal probes Thermo Scientific™ PT100 External Probe (0–400 °C) were placed on the preform, and two different isolation levels were used to prevent direct contact with the soaked net: (#A) two layers of 80% stretched medical net or (#B) two layers of cotton stockinette plus one layer of 80% stretched medical net. The employed isolation level for each measurement is reported in the text.

**Mechanical characterization.** The stiffness and mechanical behavior of the composites obtained with different formulations were first evaluated by their self-standing ability: strip samples (1 × 10 cm<sup>2</sup>) were held horizontally by an end, and it was observed if they stayed flat or curved under their own weight.

Traction tests were performed using a MesdanLab mechanical testing machine at a 10 mm min<sup>-1</sup> stroke rate on five single-layer and four double-layer composite strip samples (1 × 20 cm<sup>2</sup>; gauge length: 140 mm), 12 days after irradiation.

**Table 1** Evaluated formulation and curing parameters for composite polymerization under visible light

PhI		PhS		Single layer composite	
Name	phr	Name	phr	Irradiation time <sup>a</sup>	Stiffness <sup>b</sup>
Iod I	6	ITX	2	90 s	Not self-standing
	6	ITX	4	90 s	
	9	ITX	4	90 s	
	9	ITX	6	90 s	
Solf	4.6	<b>ITX</b>	2	<b>4.5 min</b>	Not self-standing
	4.6	ITX	4	4.5 min	
	6.9	ITX	4	4.5 min	
BTB	3	<b>ITX</b>	2	<b>230 s</b>	Not self-standing
	3	ITX	4	280 s	
	5	ITX	2	100 s	
	5	ITX	4	100 s	
T67	2.1	<b>ITX</b>	2	<b>50 s</b>	Self-standing (stiff)
	2.1	ITX	4	130 s	
	4.2	ITX	2	50 s	
	4.2	ITX	4	150 s	
Solf	4.6	C	2	6 min	Self-standing (quite stiff)
	4.6	C	4	9 min	
	6.9	C	4	9 min	

<sup>a</sup> Irradiated with white broad band light (Hamamatsu lamp) with an intensity of 130 mW cm<sup>-2</sup>. <sup>b</sup> Composites' stiffness describes the PhI/PhS class, and the stiffer composite for each combination is reported in bold.



Elastic modulus was evaluated as the slope of the linear part of stress-deformation curves (linear fit  $R^2 > 0.99$ ); the Yield Stress was calculated with the 0.2% offset method, and the Ultimate tensile strength (UTS) was evaluated as the maximum stress sustained. The average value and the standard deviation were calculated for each parameter and the group. The properties ( $P$ ) variation between double-layer (DL) and single-layer (SL) composite was evaluated by eqn (3).

$$\text{Properties variation} = \left( \frac{P_{\text{DL}} - P_{\text{SL}}}{P_{\text{SL}}} \right) \times 100 \quad (3)$$

Three-point bending tests were performed using a Zwick Z005 TN mechanical testing machine at a stroke rate of 2 mm min<sup>-1</sup>, with a support span of 100 mm. The tests were performed on different materials two months after the preparation of the cylindrical samples (diameter: 5 cm, length: 25 cm). The tested samples are (i) five double-layer composite samples, (ii) one sample of POP, and (iii) one of FGC. Photocured composite samples were performed with a two-cycle load. The Initial Stiffness was evaluated as the slope of the linear part of force-deformation curves (linear fit  $R^2 > 0.96$ ), and the Yield Force was assessed using a 0.25 mm offset method, as performed by Zmurko *et al.*<sup>6</sup>

**Harsh condition exposure.** Composite double-layer cylindrical samples were exposed to harsh environments for two hours: direct sun exposure (room temperature, 40% RH), cold or hot humid environment (cold: 5 °C, 65–70% RH; hot: 40 °C, RH 100%) and soaked in water (room temperature). The mass variation was calculated for 24 hours using eqn (4).

$$\text{MV}\% (t) = \left( \frac{m_t - m_0}{m_0} \right) \times 100 \quad (4)$$

where  $m_0$  is the sample mass before the test and  $m_t$  is the mass at time  $t$ .

## Results

In view of developing a photocurable soft cast, the first aspect that should be investigated is the matrix composition, which basically determines the final mechanical properties as well as the preparation time. Having selected CE as a reference matrix, six photoinitiators were then tested (composition and curing parameters are reported in Table S1†), evaluating their ability to provide efficient photopolymerization and to produce self-standing composites with medical net impregnation. All those tests were first performed with a UV light source because this radiation allows efficient photoinitiation with the employed photoinitiators, bringing a fast polymerization process.<sup>24,25</sup> The results, summarized in Table S1,† show that only four of them fulfilled the set criteria; consequently, those were employed in the following experiments, which will be carried out using a less hazardous radiation than UV for human skin.<sup>26–28</sup> For this reason, visible broad band white light and LED light at 410–420 nm (ad-hoc design lamp described in the Supporting Info) were employed. On the other

hand, to use such light sources, it was necessary to shift the absorption and the photoreactivity of the formulations towards higher wavelengths; therefore, different photosensitizers were studied, because they absorb less energetic photons, and transfer the energy to the photoinitiator, to initiate the polymerization.<sup>17,23,24,29</sup> In particular, two sensitizers were studied, camphorquinone and ITX, performing preliminary photopolymerization tests (results are summarized in Table S2†). Not all the combinations of PhI/PhS were suitable for photopolymerization activated in the visible range; in particular, formulations containing camphorquinone led to a slow or not-efficient polymerization in combination with all the PhI tested except with Sulf PhI. On the other hand, ITX showed good and fast polymerization in all the tested combinations, and the absorption shift was also confirmed by the UV-visible spectra reported in Fig. 1a.

After preliminary testing, the most promising formulations were tested to impregnate the medical net (Table S2†). Noteworthy, different formulations were prepared by changing the components' amount, aiming at optimizing the polymerization process and evaluating their effect on the composite stiffness. Table 1 reports the formulations tested, curing parameters and the obtained results. The composites based on Iod I/ITX, BTB/ITX, and Solf/ITX were demonstrated to be flexible after curing, indicating that those are not suitable for the application as photocurable casts. Instead, the systems T67/ITX and Solf/C allowed the production of composites with promising rigidity; among the tested combinations, one with 2.1 T67/2 ITX appeared to be the most rigid. It must be noted that the differences between the samples were easily distinguishable just by handling them, therefore this preliminary screening was merely qualitative. Conversely, mechanical testing was performed only on the final formulation, as detailed later. The stretchability of the medical net used determines another important parameter in designing composites

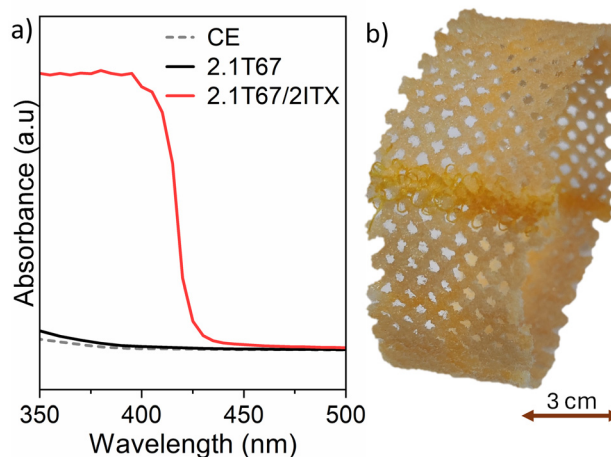


**Fig. 1** (a) UV-visible spectra of CE-based formulation with and without additives; (b) picture of a 2.1 T67/2 ITX composite cylindrical sample with a net's stretching of +80%.





for the application of orthopedic casts. This is because the net's stretching modifies the mesh size, which determines a variation in the filled/void ratio of the composite's cross-section; characteristics such as breathability and stiffness are both affected by that parameter, even if there is an opposite relation, and this peculiar behavior can be exploited to customize the rigidity in different cast sections, fitting at best the specific requirements. For this reason, a last screening evaluation was performed and aimed at assessing the more suitable net stretching, as a trade-off between stiffness and breathability. Four different 2.1 T67/2 ITX composite samples were prepared with different stretching of the net (+26%, +46%, +80%, +130%). Self-standing tests indicate that a +130% stretching was too high, with a loss of rigidity. Consequently, 80% was selected as the standard stretching level for the following tests and considerations, since it was the highest that guaranteed promising mechanical performance. A photocured sample with this stretching level is reported in Fig. 1b.

Having fixed the optimum conditions (2.1 T67/2 ITX formulation, stretching level of 80%), the polymerization process was studied and characterized in detail. To this aim, a visible broad band white light source (Hamamatsu lamp) was used, and the conversion degree (CD) was followed by means of FT-IR analyses. Furthermore, in these tests, both single- and double-layer specimens were studied, to evaluate the effect of the soft cast thickness in the photopolymerization process.

Table 2 summarizes the testing parameters and the CD (spectra reported in Fig. S1 and S2†). The obtained CDs range between 66% and 96% on the directly irradiated surface, depending on the curing conditions. As expected, the CDs of the two sides (the directly irradiated and the opposite ones) are consistently different in the samples according to their thickness, with a measured decrease of CD ranging from −8% (single layer) to −24% (double layer). This is obviously due to the light absorption along the composite thickness and this difference is more evident in the double-layer composite (#Double) since the increased thickness limits the light penetration and hinders the polymerization. Moreover, single-layer composites were produced with two energy doses (#Single\_LD – low dose- and #Single\_HD – high dose), and they resulted in a significant difference in the perceived stiffness. This difference reflects the difference in their CDs (Table 2), which are 88–96% in the latter vs. only 66–77% in the former.

**Table 2** Curing parameters and CD of 2.1 T67/2 ITX composites samples

Sample name	No. of layer (–)	Light intensity (mW cm <sup>−2</sup> )	Irradiation time (s)	CD <sup>a</sup> (%)	
				DI <sup>b</sup>	NI <sup>c</sup>
#Single_LD	1	40	50	77	66
#Single_HD	1	130	50	96	88
#Double	2	130	180	66	50

<sup>a</sup> FT-IR measurement performed 1 hour after irradiation. <sup>b</sup> Directly irradiated side. <sup>c</sup> Not irradiated (opposite side to the irradiated one).

Moreover, epoxy resins undergo a well-known phenomenon known as *dark curing*, which consists of the evolution of polymerization reaction also after irradiation. This is related to the fact that cationic polymerization is a semi-living polymerization, in which final conversion is determined by chain mobility rather than termination mechanisms.<sup>18,22,23,41,42</sup> Consequently, the CD was monitored for one month on the already analyzed specimens (Fig. 2a and Table S3,† and spectra in Fig. S1 and S2†). The results indicate that, although in some curing scenarios limited CD was reached 1 hour after the irradiation, all the tested cases showed a CD higher than 80% after 6 hours and higher than 89% in 1 month. Interestingly, the investigations showed that the difference between the two sides of the specimens tends to disappear, meaning that polymeric characteristics tend to be homogeneous with time. On the other hand, differences depending on the energy dose were still evident after 1 month (#Single\_LD: 89%, #Single\_HD: 97–100%), confirming that an optimization of the curing parameters is crucial to obtain rigid composites to be employed as orthopedic casts. Related to the double-layer sample, observing the CDs evaluated 1 hour after irradiation on both surfaces, their values indicated low polymerization, even lower than the #Single\_LD sample. However, after 6 hours, the measured CD overcame those values, becoming more similar to #Single\_HD. Consequently, despite the polymerization being hindered by the increased thickness, the curing conditions employed led to a proper reaction. However, in the double-layer composites, the irradiation time is strongly increased compared to single-layer samples, therefore two is the maximum number of evaluated layers in this work, to avoid an extremely long curing process.

Unfortunately, uncured resins could potentially cause skin irritation. To prevent this, the presence of an insulating layer is suggested, it is useful also to avoid the adhesion of the composite on the skin and to control the temperature perceived by the user. However, this part will be better discussed later in the text.

In addition, it is well-known that epoxy curing is an exothermic process; therefore, the exothermicity of the reaction can give an indication of the photopolymerization process but, for the envisaged application, it can be harmful to the human body. For this reason, the temperatures generated on the irradiated surface during the polymerization were monitored employing a thermal camera (Fig. 2b). Those measures highlight the effect of the light dose on the single-layer composite's polymerization, demonstrating that when the intensity is higher, the polymerization process is faster, as confirmed by the high developed temperature. In the double-layer sample, the effective activation was confirmed by the temperatures developed, which are consistently higher than the ones developed in #Single\_LD, and more similar to #Single\_HD. These results are consistent with the previously discussed increased CDs, so temperature monitoring was revealed to be a proper test to estimate the ongoing polymerization reaction.

FT-IR analyses and temperature measurements demonstrated that an optimization of the curing parameters is crucial



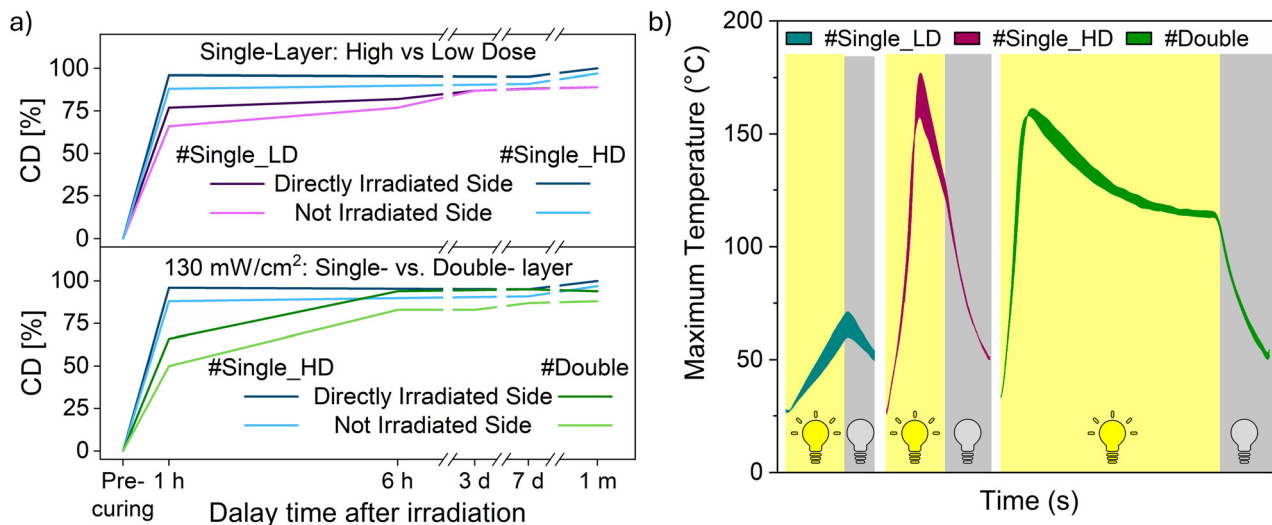


**Fig. 2** (a) Change in the conversion degree over one month, and (b) maximum temperatures developed on the irradiated side of 2.1 T67/2 ITX composites samples.

to obtaining rigid composites to be employed as orthopedic casts. This procedure aimed to match the applications' requests as the orthopedic cast; namely, low curing time and high polymerization efficacy were pursued. For this reason, the curing conditions were selected for broad band visible light sources in order to have a CD of (at least) 85–90%, 6 hours after irradiation (Table S5†). It is important to highlight that, even if low conversion degree may be obtained right after the irradiation, dark curing will ensure complete polymerization in a few hours. The optimized curing parameters are reported in Table S4.† This procedure was also conducted for another light source, solar simulator, due to the necessity of fabricating specimens with dimensions sufficient for following characterization; in fact, the Hamamatsu lamp has a spot size of around 1–2 cm<sup>2</sup> at the required intensity, which is unsuitable for the production of homogeneous bigger samples for mechanical testing.

Consequently, mechanical properties were evaluated. Tensile tests were performed on single- and double-layer composites cured with the optimized curing conditions, and relevant results are reported in Table 3 and Fig. S4.† As predicted, the double-layer composites show an improvement in their mechanical properties compared to single-layer composites: the elastic modulus reaches an average value of 221 ± 28 MPa vs. 187 ± 51 MPa; thus, an improvement of +18% is obtained. Furthermore, yield stress was measured respectively as 1.78 ± 0.12 vs. 1.4 ± 0.24 MPa, with an improvement of +27%. Interestingly, after increasing the number of layers, the dispersion of the values obtained for elastic modulus and yield stress parameters decreased by 45–50%, meaning that the reliability of the composite improved. Comparing those results to Plaster of Paris and Fiber Glass performance reported in the literature, the elastic modulus of the photocured double-layer composite is considerably lower than POP (6-layer samples: 2590 ± 708 MPa), while it has the same order of magnitude of

**Table 3** Elastic moduli, ultimate tensile strength, and yield strength resulting from tensile tests on single- and double-layer composites

		Composites <sup>a</sup>		
		Single-layer <sup>b</sup>	Double-layer <sup>c</sup>	Single- vs. double-layer variation
E [Mpa]	Average	187	221	+18%
	Stand. dev.	51	28	–45%
UTS [Mpa]	Average	1.43	1.88	+31%
	Stand. dev.	0.23	0.12	–48%
Yield stress [Mpa]	Average	1.40	1.78	+27%
	Stand. dev.	0.24	0.12	–50%

<sup>a</sup> Irradiated with a solar simulator (curing parameter in Table S4†) and tested 12 days after irradiation. <sup>b</sup> 6 samples were tested. <sup>c</sup> 5 sample tested.

FGC despite the lower layers' number (4-layers FGC samples: 316 ± 15 MPa), which revealed to be enough for the orthopedic application.<sup>43</sup>

Beyond tensile, three-point bending tests were also performed. To assess a solicitation scenario that was more similar to the real one, the measurements were performed on cylindrical double-layer samples having a dimension comparable to a real limb cast. Nevertheless, the fabrication of such specimens needed a last modification of the irradiation set-up: the sun simulator was replaced with an *ad-hoc* designed lamp that can irradiate larger surfaces and be portable, thus making it more suitable in view of orthopedic uses. More details are reported in the ESI,† and the optimized curing conditions with this lamp are reported in Table S9.† The reaction of the samples described in Table S8† was followed by monitoring the external temperatures, as reported in Fig. S6.† The values obtained



show a significant difference between each irradiation step (three were required to ensure covering the whole cylinder surface), with a consistent reduction of the maximum temperature reached in the last step. This can be related to the fact that the composite is already partially polymerized in the overlapping areas, especially in the last step of the Double\_LED\_210s samples.

Once those specimens were produced, whose pictures are reported in Fig. 3a, three-point bending tests were performed in order to compare the properly cured specimens (Double\_LED\_210s) with the ones obtained with non-optimal parameters (samples Double\_LED\_90s). Load vs. deformation curves are shown in Fig. 3b and Fig. S7b,† while the mechanical properties are summarized in Table S10.† Samples Double\_LED\_210s\_#1, Double\_LED\_210s\_#2, and Double\_LED\_210s\_#3 show an initial stiffness of  $5.21 \pm 1.08 \text{ N mm}^{-2}$  and yield stress of  $2.52 \pm 0.56 \text{ N}$ , confirming, as expected, better mechanical properties than those of the composites cured with non-optimal parameters (Double\_LED\_90s samples: initial stiffness:  $1.90 \pm 0.55 \text{ N mm}^{-2}$ , yield stress:  $3.44 \pm 0.79 \text{ N}$ ). Interestingly, three-point bending tests on samples Double\_LED\_210s\_#4 and Double\_LED\_210s\_#5 gave results similar to those on Double\_LED\_90s samples, initial stiffness:  $2.26 \pm 0.12 \text{ N mm}^{-2}$  and yield stress:  $3.28 \pm 0.24 \text{ N}$ ; to better understand this phenomenon, their external temperatures monitoring results were recalled (Fig. S6†). Noteworthy, those particular specimens did not reach the high temperature developed by the other Double\_LED\_210s samples, probably due to inhomogeneous resin distribution. This confirms the correlation between the external temperature developed, and consequently the extent of polymerization, and the composites'

mechanical properties. To describe in detail, Double\_LED\_90s samples show similar and low maximum temperatures to Double\_LED\_210s\_#4 and Double\_LED\_210s\_#5 (1<sup>st</sup> step:  $<130^\circ\text{C}$ , 2<sup>nd</sup> step:  $<90^\circ\text{C}$ , 3<sup>rd</sup> step:  $<60^\circ\text{C}$ ), and this result in similar weak behavior in the bending test (initial stiffness:  $1.34\text{--}2.38 \text{ N mm}^{-2}$ ). Instead, samples Double\_LED\_210s\_#1 and Double\_LED\_210s\_#2 developed higher temperatures in both the first and the second steps (1<sup>st</sup> step:  $<180^\circ\text{C}$ , 2<sup>nd</sup> step:  $<130^\circ\text{C}$ , 3<sup>rd</sup> step:  $<60^\circ\text{C}$ ), resulting in stronger composites (Initial Stiffness:  $4.95\text{--}6.65 \text{ N mm}^{-2}$ ). Confirming this trend, samples Double\_LED\_210s\_#3 developed intermediate temperatures (1<sup>st</sup> step:  $<130^\circ\text{C}$ , 2<sup>nd</sup> step:  $<130^\circ\text{C}$ , 3<sup>rd</sup> step:  $<60^\circ\text{C}$ ) and resulted in intermediate strength (initial stiffness:  $4.04 \text{ N mm}^{-2}$ ).

Overall, well-cured double-layer cylindrical samples show an initial stiffness of  $5.21 \pm 1.08 \text{ N mm}^{-2}$  and a Yield stress of  $2.52 \pm 0.56 \text{ N}$ , and those values were compared to POP and FGC samples prepared by a registered orthopedic technician with the proper amount of layer required for the materials ( $>6$  for POP and  $>4$  for FGC) and tested under the same conditions. Their initial stiffness resulted in  $333 \text{ N mm}^{-2}$  and  $72 \text{ N mm}^{-2}$  respectively for POP and FGC, while the Yield stress is  $23 \text{ N}$  and  $40 \text{ N}$ ; those values are quite consistent with literature data, with a reasonable variation related to the operator.<sup>6</sup> Despite the lower mechanical properties shown by the photocured composite presented here, its application as a rapid orthopedic cast is still appealing because it shows similar bending behaviors to a Soft Cast applied in a higher number of layers (4–10 layers Initial Stiffness:  $<10 \text{ N mm}^{-2}$ , 4–6 layers Yield stress  $<10 \text{ N}$ ).<sup>6</sup> Moreover, the presented photocured composites showed an additional advantage compared to the con-

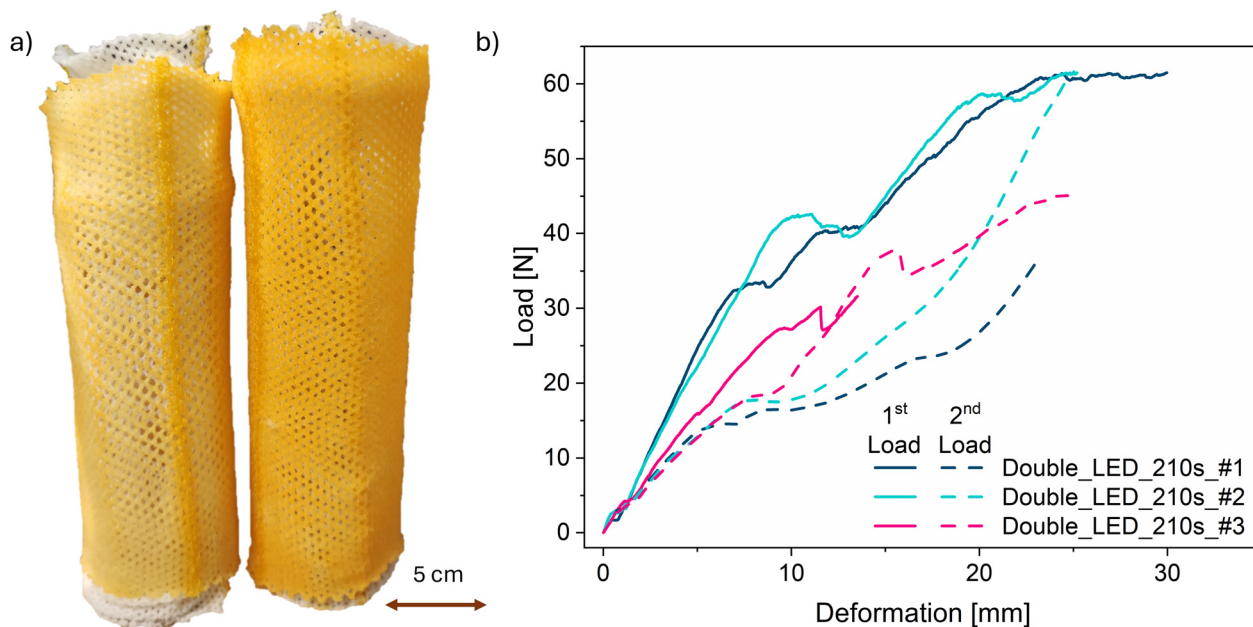


**Fig. 3** (a) Picture of 2.1 T67/2 ITX double-layer composites; (b) load vs. deformation of the cured cylindrical double-layer composites irradiated with LED lamp, including multiple testing.



ventional casting technique, since they recover their initial shape after the load removal, while POP and FGC cast are irreversibly deformed. For this reason, the analyzed specimens were tested with a second cycle of load application in the same three-point bending test condition right after the first load cycle. Interestingly, they preserve  $76 \pm 13\%$  of their initial stiffness despite the failure in the test's first cycle, meaning that the cast will still provide support to the injured part in the case of traumatic events.

However, as already mentioned in this study, the curing of the epoxy resins is an exothermic process, and the developed temperature can be harmful for the application on human skin.

External temperature monitoring has been previously discussed, but it is reasonable to assume that the perceived temperature will be that of the side of the soft cast closer to the skin, which is not the side previously analyzed. For this reason, the internal temperatures developed were monitored through thermal probes directly applied on the preform during the polymerization of single-layer cylindrical composites. These measures were conducted in two different thermal insulating conditions: the first scenario consists of 2 layers of clean medical nets having a stretching of +80%, not impregnated with resins (#A). This option should give a minimum insulating level, simply preventing skin irritation and adhesion with the composite. The second scenario was instead designed with 2 layers of cotton stockinette and a layer of clean medical net (stretching level of 80%) to keep the stockinette in the right position and facilitate the application of the soak layer and hopefully provide a partial thermal insulation (#B). The results of those scenarios are reported in Fig. 4a and b.

In scenario #A, the peak temperatures developed are under  $85^\circ\text{C}$ , which are considerably lower than the temperatures

reached externally ( $180\text{--}200^\circ\text{C}$ ). However, despite this drop in temperatures, those values are still too high for applications on the human skin. For this reason, the second insulation scenario was analyzed, and the maximum temperature measured by the thermal probes was  $53\text{--}59^\circ\text{C}$ . In summary, in the second configuration (i) the reached maximum temperature decreases by 12–30% ( $60\text{--}85^\circ\text{C}$  vs.  $53\text{--}59^\circ\text{C}$ ), (ii) the time needed to reach the maximum temperature increases by 45–67% ( $55\text{--}60\text{ s}$  vs.  $80\text{--}100\text{ s}$ ), (iii) the period in which the preform stay at temperatures higher than  $40^\circ\text{C}$  slightly increases ( $220\text{ s}$  vs.  $240\text{ s}$ ). The second configuration was also tested with double-layer composites (Fig. 4c). Also in this case, the maximum temperatures developed are around  $53\text{--}58^\circ\text{C}$  as for the single-layer composite, but the period in which the preform stays at temperatures higher than  $40^\circ\text{C}$  is more than 6 minutes. Analyzing those results, it clearly emerges that a more efficient insulation must be designed in view of the application of this study.

Finally, a last preliminary investigation was conducted to assess the composite's response to harsh conditions, such as direct sun exposure, cold or hot humid environments, and soaking in water, because those conditions can frequently occur if the composite is applied as an orthopedic cast. Cylindrical double-layer samples were exposed to such conditions for two hours and then the mass variation was monitored for 24 hours, as well as the samples' perceived stiffness. No rigidity changes were registered, and the mass variation, summarized in Table S11† indicates that only water immersion caused a significant weight increase; still, most of the absorbed water can be eliminated in one hour and completely removed in less than one day.

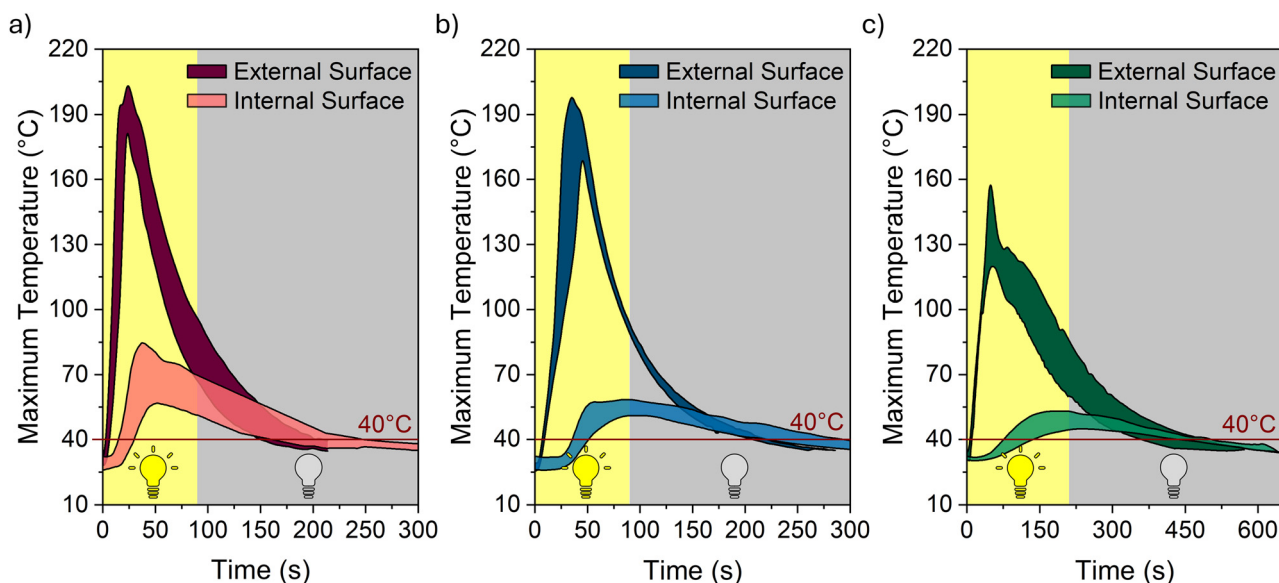


**Fig. 4** Maximum temperatures measured on the external and internal surface during the curing through LED lamp of (a) a cylindrical single-layer composite with the insulation level #A; (b) cylindrical single-layer composite with the insulation level #B; (c) cylindrical double-layer composite with the insulation level #B.





## Conclusions

In this work, photocurable polymeric composites with promising properties for the application as orthopedic rapid soft casts were successfully developed, showing an initial stiffness similar to other soft casts even if applied in a lower number of layers (composites studied here: 2 layer – initial stiffness of  $5.21 \pm 1.08 \text{ N mm}^{-2}$  | commercially available soft cast: 4–10 layers – Initial Stiffness:  $<10 \text{ N mm}^{-2}$ )<sup>6</sup>. Compared to the commercially available photocurable casts, two main innovations are introduced, and they consist of the use of a transversally stretchable tubular medical net and the use of an epoxy-based resin as the photocurable matrix. Both those elements are commercially available, and epoxy photocuring does not suffer from oxygen inhibition; therefore, the impregnation can be easily performed on demand without particular technical skills, and irradiation can be performed in every condition, including emergencies. The photoinitiator T67 and the photosensitizer IXT were selected as the best combination for the monomeric formulation to achieve a fast polymerization and shift the absorption from the UV range to the visible range, thereby preventing skin damage caused by UV light; while the curing parameters were optimized to reach a high conversion degree, resulting in a composite with suitable rigidity for the application. Additionally, the composite's stiffness can be tuned by modifying the number of medical net layers and their stretching to better meet specific requirements.

One limitation identified in this study is the elevated temperature developed during the photocuring process, which may be potentially harmful to the user. Temperatures of up to 200 °C are reached on the irradiated surface, however, they decrease significantly across the device thickness, down to under 85 °C on the skin side. Clearly, this temperature is still not acceptable for patients, and the use of an insulating layer was suggested. The presence of this layer allows to reduce the maximum internal temperature by a further 12–30%; however, to ensure the composite's suitability for real applications, a more efficient thermal insulation system must be designed. Additionally, this insulating layer also prevents contact between the skin and the uncured resin, avoiding undesired effects on the skin.

To conclude, the approach proposed simplifies the application process compared to conventional techniques, resulting in casts that are light, breathable, and easy and fast to apply.

## Data availability

The data supporting this article have been included as part of the ESI.†

## Conflicts of interest

There are no conflicts to declare.

## Acknowledgements

The work of B. T. was carried out with the support of the National Recovery and Resilience Plan (NRPP), DM 351. The work of I. R. received funding from the FSE REACT-EU – PON Ricerca e Innovazione 2014-2020. This manuscript reflects only the authors' views and opinions, neither the European Union nor the European Commission can be considered responsible for them.

## References

- 1 C. Ekanayake, J. C. P. H. Gamage, P. Mendis and P. Weerasinghe, *Heliyon*, 2023, **9**, e13640.
- 2 M. Prior and S. Miles, *Emerg. Nurs.*, 1999, **7**, 33.
- 3 M. A. Halanski, A. D. Halanski, A. Oza, R. Vanderby, A. Munoz and K. J. Noonan, *J. Bone Jt. Surg.*, 2007, **89**, 2369.
- 4 H. Sharma and D. Prabu, *J. Clin. Orthop. Trauma.*, 2013, **4**, 107.
- 5 C. Hui, E. Joughin, A. Nettel-Aguirre, S. Goldstein, J. Harder, G. Kiefer, D. Parsons, C. Brauer and J. Howard, *Can. J. Surg.*, 2014, **57**, 247.
- 6 M. G. Zmurko, S. M. Belkoff and J. E. Herzenberg, *Orthopedics*, 1997, **20**, 693.
- 7 R. White, J. Schuren and D. R. Konn, *Clin. Biomech.*, 2003, **18**, 19.
- 8 C. Witney-Lagen, C. Smith and G. Walsh, *Injury*, 2013, **44**, 508.
- 9 P. K. Chhatrala, M. Pawar, C. Sapovadiya, H. Prajapati and S. Makwana, *A Polysiloxane orthopedic immobilizer*, 2022.
- 10 N. Nakasugi and Y. Matsumoto, *Orthopedic photo-curable fixing material*, 2007.
- 11 K. Kubushiro, *Photocurable flexible orthopedic bandage*, 1977.
- 12 R. Perry and J. Nemcek, *Photocurable resin impregnated fabric for forming rigid orthopaedic devices and method*, 1975.
- 13 C. J. Buck and B. Height, *Visible light cured orthopedic polymer casts*, 1985.
- 14 D. C. Garwood and H. Taw, *Photocurable contour conforming splint*, 1976.
- 15 J. A. Corvi and D. C. Garwood, *Ultraviolet light curable orthopedic cast material and method of forming an orthopedic cast*, 1975.
- 16 S. Vasilca, M. Virgolici, M. Cutrubinis, V. Moise, P. Mereuta, R. Sirbu and A. V. Medvedovici, *Polym. Adv. Technol.*, 2024, **35**, e6381.
- 17 F. Schnetz, I. Knysh, D. Jacquemin, S. A. Andaloussi, M. Presset, S. Lajnef, F. Peyrot and D.-L. Versace, *Polym. Chem.*, 2024, **15**, 1377.
- 18 O. Škola, B. Jašúrek, D. Veselý and P. Němec, *Prog. Org. Coat.*, 2016, **101**, 279.
- 19 G. Gershoni, H. Dodiuk, R. Tenne and S. Kenig, *J. Compos. Sci.*, 2023, **7**, 41.
- 20 F. Bian and S. Lin, *Pigm. Resin Technol.*, 2023, **53**, 650.



- 21 J. V. Crivello, *J. Polym. Sci., Part A: Polym. Chem.*, 1999, **37**, 4241.
- 22 S. Shen, X. Liu, Y. Shen, J. Qu, E. Pickwell-MacPherson, X. Wei and Y. Sun, *Adv. Opt. Mater.*, 2022, **10**, 2101008.
- 23 S. Zhong, D. Armstrong, M. Hetrich and J. Kadoko, Formulation, Curing Kinetics and Properties of Photocurable Epoxy Resins, 2023 IEEE Electrical Insulation Conference (EIC), Quebec City, QC, Canada, 2023, pp. 1–4, DOI: [10.1109/EIC55835.2023.10177309](https://doi.org/10.1109/EIC55835.2023.10177309).
- 24 S. Shi, C. Croutxé-Barghorn and X. Allonas, *Prog. Polym. Sci.*, 2017, **65**, 1.
- 25 R. Liu, Y. Xu, L. Wang, F. Zhang, P. Chen, Y. Li and Y. Chen, *Polym. Bull.*, 2021, **78**, 4849.
- 26 J. Xiang, P. Huang, X. Mao, Z. Yu, J. Lin, S. Xie, Y. Gu, Z. Wang and Z. Zheng, *Polym. Bull.*, 2024, **81**, 10135.
- 27 E. R. Gonzaga, *Am. J. Clin. Dermatol.*, 2009, **10**, 19.
- 28 Y. Xu, B. Zhang, Z. Xu, W. Ye, B. Guo, J. Zhuang, C. Hu, B. Lei, G. Hu and Y. Liu, *Dyes Pigm.*, 2024, **225**, 112060.
- 29 E. W. Nelson, T. P. Carter and A. B. Scranton, *J. Polym. Sci., Part A: Polym. Chem.*, 1995, **33**, 247.
- 30 C. Li, T. Li, X. Cai and X. S. Sun, *Polymer*, 2016, **107**, 19.
- 31 N. Gao, W. Liu, Z. Yan and Z. Wang, *Opt. Mater.*, 2013, **35**, 567.
- 32 I. D. Robertson, M. Yourdkhani, P. J. Centellas, J. E. Aw, D. G. Ivanoff, E. Goli, E. M. Lloyd, L. M. Dean, N. R. Sottos, P. H. Geubelle, J. S. Moore and S. R. White, *Nature*, 2018, **557**, 223.
- 33 T. Zhang, N. Xu, W. Yin, D. Liu, C. Liu and M. Lang, *Mater. Today Commun.*, 2024, **40**, 109494.
- 34 J. Staal, E. Smit, B. Caglar and V. Michaud, *Compos. Sci. Technol.*, 2023, **237**, 110009.
- 35 M. Sangermano, A. D'Anna, C. Marro, N. Klikovits and R. Liska, *Composites, Part B*, 2018, **143**, 168.
- 36 C. Noè, M. Hakkarainen, S. Malburet, A. Graillet, K. Adekunle, M. Skrifvars and M. Sangermano, *Macromol. Mater. Eng.*, 2022, **307**, 2100864.
- 37 Infrared and Raman Characteristic Group Frequencies: Tables and Charts, ed. G. Socrates, The University of West London, Middlesex, U.K., J. Wiley and Sons: Chichester, 3rd edn, 2001.
- 38 F. Boey, N. Chia, S. Rath and M. Abadie, *J. Appl. Polym. Sci.*, 2001, **82**, 3099.
- 39 U. Soydal, *World Academy of Science, Engineering and Technology, International Journal of Chemical, Molecular, Nuclear, Materials and Metallurgical Engineering*, 2016.
- 40 M. G. González, J. C. Cabanelas and J. Baselga, in *Infrared Spectroscopy - Materials Science, Engineering and Technology*, ed., T. Theophanides, InTech, 2012.
- 41 M. Sangermano, N. Razza and J. V. Crivello, *Macromol. Mater. Eng.*, 2014, **299**, 775.
- 42 S. Kaalberg and J. L. P. Jessop, *J. Polym. Sci., Part A: Polym. Chem.*, 2018, **56**, 1436.
- 43 W. M. Mihalko, A. J. Beaudoin and W. R. Krause, *J. Orthop. Trauma*, 1989, **3**, 55.

